Chapter III

DSC AND SMALL ANGLE X-RAY SCATTERING STUDIES ON SMECTIC AND NEMATIC PHASES OF TWO BI-SCHIFF'S BASES

Part of this work has been published in *Mol. Cryst. Liq. Cryst.*, **265**, 249 (1995)

3.1 INTRODUCTION

Liquid crystals with low melting points are used in various electro-optical devices. High-temperature melting liquid crystals, therefore, attracted little attention till it was suggested that such systems might be used in gas-liquid chromatography (GLC). Use of liquid crystals in GLC was reviewed by Kelker and Von Schivizhoffen [1] and Schroeder [2]. The main aim was to use high-melting nematic liquid crystals for the gas-liquid chromatographic separation of geometric isomers of various systems like underivatized steroid epimers [3], drug isomers [4], 3-5 ring polycyclic aromatic hydrocarbon (PAH) isomers [5] etc. which is not attainable by conventional GLC liquid phases. With this aim Janini *et al.* [6] synthesised the di-Schiff's base compound N, N′ –Bis (p-methoxybenzylidine)-α, α′ -bi-p-toluidine (BMBT) and found that it can be used in the analysis of high-boiling solute classes having a broad based interest to biochemical and ecological research. For example, separation of PAH isomers by GLC using BMBT has direct application in carcinogenesis research and in environmental evaluation of human exposure to PAH. They later found that the butoxy member of the series (BBBT) is more effective than BMBT [7,8]. General conclusion was that for members of a homologous series, the higher the temperature T_{NI} and the order parameter $\langle P_2 \rangle$, the more effective it is in GLC separation. BMBT, BBBT and several other members of the series were studied by Janini *et al.* [6-8] to determine the transition temperatures by optical microscopy and thermodynamic parameters at transition points by DSC study, phases were identified by the optical textures. To the best of our knowledge no X-ray diffraction study on the compounds has been done so far. We have, therefore, undertaken the study of BMBT and BBBT by small angle X-ray scattering technique to determine various physical and molecular properties in both the smectic and nematic phases. Molecular and crystal structure of the compound BBBT was also reported from our laboratory earlier [9]. Packing of the molecules in the liquid crystalline as well as in the crystalline state has been discussed. Different properties of BMBT and BBBT have been compared with other structurally related compounds like mono- and di-Schiff's bases.

3.2 EXPERIMENTAL

The title compounds, BMBT and BBBT, were obtained from Eastman Kodak and used without further purification. Phase transition temperatures were determined by studying textures under polarizing microscope (150X). Mettler FP82 hot stage and FP80 control system were used.

Small angle X-ray photographs of both non-aligned and magnetically aligned samples were taken throughout the mesomorphic range. A high temperature camera, described in Chapter II, was used. The sample was taken in Lindemann glass capillary of ~ 1.0 mm diameter and a temperature controller (Indotherm 401-D2) was used to control the temperature within ±0.5°C. We tried to get monodomain sample in smectic phase by very slow and regulated cooling from isotropic to smectic phase using only the capillary surface effect and also applying magnetic field of 0.5 Tesla. Attempt was also made to align the sample by slow heating to smectic phase in presence of magnetic field. But only partial alignment could be achieved. All photographs were taken with X-rays perpendicular to the magnetic field direction. In order to determine various parameters the photographs were scanned linearly and circularly by an optical densitometer (Carl Zeiss, Jena, Model MD100). Details of the experimental procedure have been described in Chapter II.

3.3 RESULTS AND DISCUSSIONS

An unspecified variety of mosaic texture in the smectic region and marbled texture in the nematic phase were observed in texture study. Nematic droplets were observed at N-I transition both during heating and cooling. Pre-transition effect was observed both before Cr-Sm and N-I transitions. Structural formula of the compounds, observed phase sequence with transition temperatures (in °C) and thermodynamic parameters are given below:

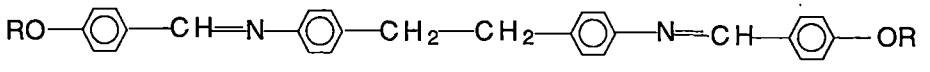

BMBT:	Cr	179.3 (181) ⟷		N	309.4 (337) ⟷	I
(R=CH_3)		145.1				
ΔH (kJ/mole)		**50.4 (43.5)**			**1.1 (7.2)**	
ΔS (J/mole.K)		**111.4 (96.0)**			**1.9 (11.7)**	

BBBT :	Cr	159.0(159) ⟷		Sm	188.0 (188) ⟷	N	293.0 (303) ⟷ I
(R=C_4H_9)		145.0			172.0		
ΔH (kJ/mole)		**26.53 (24.7)**			**12.04 (12.2)**		**5.01 (8.5)**
ΔS (J/mole.K)		**61.39 (57.2)**			**26.11 (26.5)**		**8.85 (14.7)**

Transition temperatures and the thermodynamic parameters at the transition points obtained by Janini *et al.* [6,7,8] are given within parentheses for comparison. It is observed that the transition temperatures, determined from texture studies, agreed with reported values except T_{NI} which was 28° (for BMBT) and 10° (for BBBT) less than the reported values. Repeated observations yielded same values. Supercooling effect was also observed by us at N-Cr, N-Sm and Sm-Cr transitions which was not reported earlier. Though it is unusual to have a hysteresis effect at transitions within different mesophases but such observation has been reported recently [10]. The DSC study at a heating rate of 5°C/min, made with Mettler thermosystem FP84, showed transition temperatures almost identical to those observed by texture study. Calculated transition enthalpies (ΔH) and entropies (ΔS) during heating are shown above. Values obtained by Janini *et al.* [8] are shown within parentheses. The maximum discrepancy in thermodynamic parameters is also observed at T_{NI}. It might be noted that Janini *et al.* [7,8] made DSC study at a scan rate of 10 or 20°C/min. This high scan rate may be one of the reasons of discrepancy in T_{NI} and thermodynamic parameters. Moreover, they were not sure about the purity of the compound. Also to find the accuracy of their results they measured ΔH value at T_{NI} of PAA and found it to be 0.72 kJ/mole [8]. They observed that this was in good agreement with values reported in [11]. However, Chandrasekhar [12] quoted ΔH value at T_{NI} of PAA as 0.574 kJ/mole (measured by Arnold [13]). This is about 26% less than the measured value of Janini *et al.* [8]. For BBBT during

cooling the N-Sm transition was detected by DSC at 171.1°C as against 172.0°C by texture study; the Sm-Cr transition was observed at 120.2°C whereas by texture study the transition was observed at 145.0°C. X-ray study (described below) reveals that this was actually CrII-CrI transition, so by DSC study we could not detect Sm-Cr transition. This may not be very unusual if it is considered that the smectic phase is actually a highly ordered 'soft' crystalline state as described later.

Janini *et al.* [8] observed that the first two members of the series were pure nematogens, the next two members showed both nematic and smectic phases, members with n=5-8 showed two smectic types and a nematic region while the tenth member exhibited only one smectic phase. However, as noted earlier, they identified the phases only by texture study, so could not characterize the phases explicitly. A representative X-ray diffraction photograph of BMBT at 165°C is shown in Figure 3.1. This is a typical nematic photograph except that the inner ring is weak. X-ray photographs of BBBT in smectic phase at 160°C are shown in Figures 3.2(a) for non-aligned sample and in Figure 3.2(b) for magnetically aligned sample. From the X-ray photographs the phase apparently appears to be a crystalline phase rather than smectic. It shows two very closely spaced outer rings with 'd' values of 4.44 and 4.55 Å; there are four inner rings with 'd' spacings of 11.97, 13.55, 21.47 and 29.90 Å, not multiple of each other (Table 3.1). These data are obtained from aligned sample. Both the photographs were taken during cooling from isotropic phase. Evidently though monodomain sample could not be obtained, partial alignment could be achieved by applying magnetic field which is not expected in crystalline phase. Moreover, comparison of photographs at 158°C, one obtained during heating (Figure 3.3(a)) and the other during cooling (Figure 3.3(b)), suggests that the former photograph is in crystalline phase while the latter is in smectic phase. Since the innermost ring originates from the density variation along the smectic layers, the smectic layer thickness would be 29.90Å at 160°C.The model length of BBBT in all *trans*-conformation is found to be 34.3 Å. So the molecules are tilted within the smectic layers, the tilt angle being 29.3°. This tilt angle is found to decreases with temperature (shown later) and it is not expected in a perfect

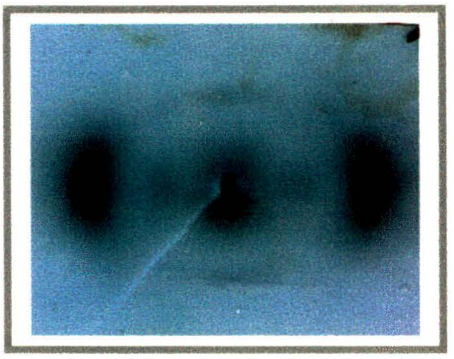

Figure 3.1 X-ray diffraction photograph of BMBT at 165°C in nematic phase.

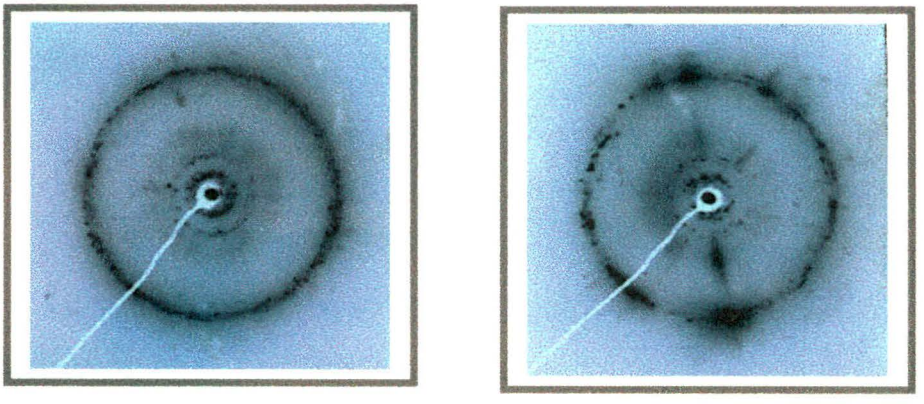

(a) (b)

Figure 3.2 X-ray diffraction photographs of BBBT in smectic phase: (a) non aligned and (b) aligned at 160°C.

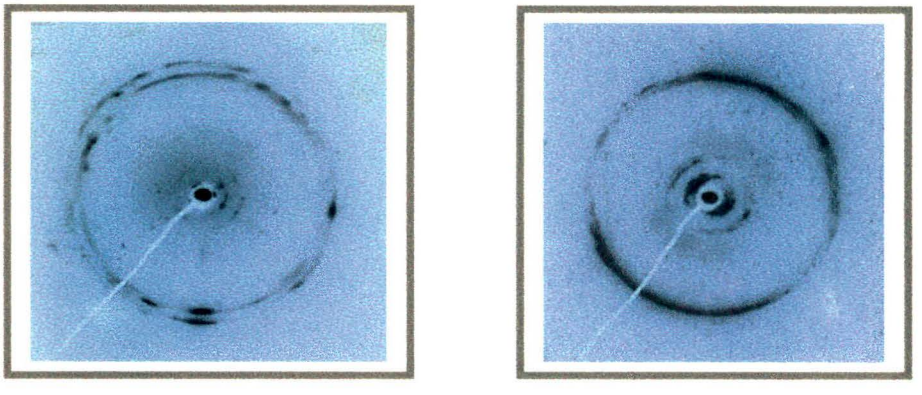

(a) (b)

Figure 3.3 X-ray diffraction photographs of BBBT at 158°C: (a) during heating and (b) during cooling.

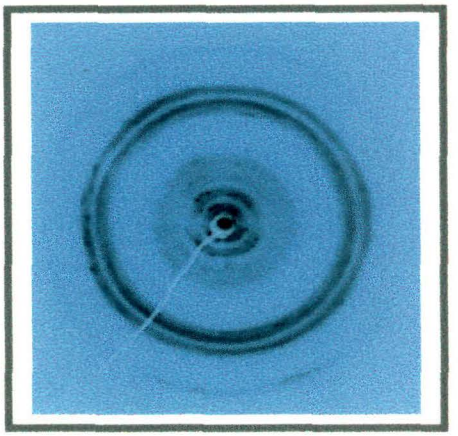

Figure 3.4 X-ray diffraction photographs of BBBT at room temperature (25 °C).

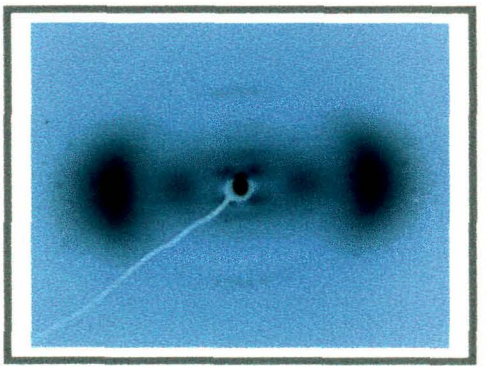

Figure 3.5 X-ray diffraction photograph of BBBT in nematic phase at 183 °C.

crystalline phase. However, presence of two closely spaced sharp outer rings indicates that there is long range positional ordering within the layers. Doucet [14] and Vertogen [15] noted the appearance of closely spaced several rings in Sm G and Sm H phases in powder pattern of TBBA and PPP. Probably, because of very high degree of thermal agitation higher order outer rings are not visible in our case. All these features along with the observed texture and DSC data suggest that the above phase is a tilted version of Crystal B or Crystal E phase. So the phase may be SmG/SmG'/SmH/SmH' which are now termed as Crystal G/J/H/K phases [16,17]. For precise identification of the phase, one, however, needs to index a photograph obtained from a mono-domain sample with X-rays parallel to the smectic layer normal. As far as the extent of positional ordering is concerned these modifications are crystalline i.e. there is long range order within and perpendicular to the smectic layers; however, the molecules are undergoing rapid reorientational motion about their long axes normally not observed in crystals[17]. So they are also called smectic like 'soft' crystals. It may be of interest to point out that Crystal G phase was observed in mono-Schiff's base compounds *p-n-alkoxybenzylidene-p'-n-alkylaniline (nO.m)* [18,19] and as mentioned before, in a pyrimidine compound 2-(4-n-*pentylphenyl)-5-(4-n-pentyloxyphenyl) pyrimidine* (PPP) [20]. Both the Crystal G and Crystal H phases were observed in directly coupled di-Schiff's base compound *Terephthalylidene-bis-(p-butylaniline)* (TBBA) [21,22].

X-ray photograph of BBBT at room temperature is shown in Figure 3.4. Measured 'd' spacings reveal that this phase is different from the crystalline phase observed at 158°C during heating (Figure 3.3(a)). Thus there are two crystalline modifications in the sample. In DSC study this CrII-CrI transition is observed at 120.2°C. Presence of two or more crystalline modifications is not uncommon in mesophase forming compounds, for example three crystalline modifications have been observed in OOBPD [23]. For many nCB and nOCB members it was observed that slow or delayed cooling gives rise to a lower melting crystalline ploymorphic form which then slowly converts into the higher melting stable crystalline structure [24-27]. These polymorphic crystalline forms result from a subtle balance of intermolecular interactions [28].

It is also observed that the diffraction photograph of BBBT at 150°C during cooling is not of smectic phase, as was expected from texture study, rather it shows Cr-II phase. The 'd' spacings obtained from this photograph are similar to those observed at 158°C during heating. Thus though the texture study indicates supercooling of the smectic phase till 145°C, but X-ray studies show that the supercooling is not extended even upto 150°C. Different container geometry, sample thickness and external alignment field in the two experimental situations may be responsible for this type of anomalous behaviour.

Aligned X-ray photograph in the nematic phase of BBBT is given in Figure 3.5. This photograph is qualitatively different from the nematic phase photograph of BMBT (Figure 3.1). In addition to the outer crescents it is observed that the inner crescent, in this case, splits into four distinct spots symmetrically about the meridional direction. Unlike the ordinary nematic phase in BMBT, this phase is, therefore, identified as skewed cybotactic nematic phase where the molecules are arranged in 'cybotactic groups' such that the ends of the rod-like molecules constitute more or less a well-defined boundary plane which is tilted to the average direction of the molecules in the group (Figure 2.6). Such phase has been observed in mono-Schiff's base compound 4O.4 [19]; in several members of the series bis-(4'-n-alkoxybenzal)-2-chloro-1,4-phenylinediamine [29-34]. Cybotactic nematic phase has also been observed by the author (and co-workers) in pentyl and octyl members (and in their binary mixtures) of the series *p-pentylphenyl-2-chloro-4-(p-pentylbenzoyloxy)-benzoate* [35] (Though a substantial amount of work was done by the author, results of this work are not presented in this dissertation since those results were presented by the first author Parimal Sarkar in his thesis).

Variations of different molecular parameters, determined from X-ray photographs, with temperature have also been studied. The outer equatorial arc in the nematic phase arises from the intermolecular distances perpendicular to the director. Finding the peak position the average intermolecular distance, D, is calculated using a modified Bragg's relation, $2D\sin\theta=1.117\lambda$, obtained on the assumption of cylindrical symmetry of the molecules [29,30]. In BMBT the D

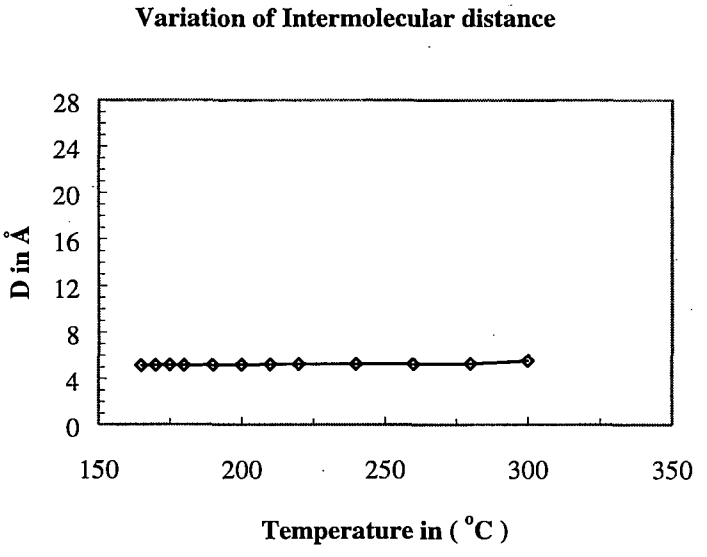

Figure 3.6 Temperature variation of D in the nematic phase of BMBT.

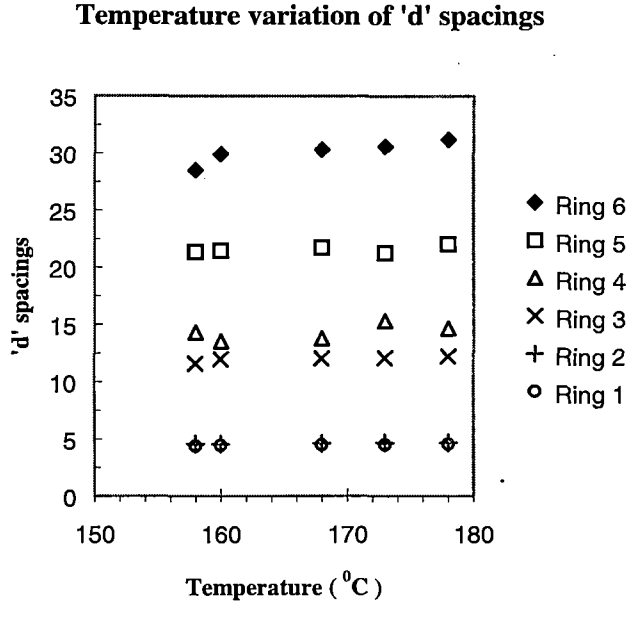

Figure 3.7 Temperature variation of 'd' spacings in smectic phase of aligned BBBT. Outermost ring is labeled as ring 1.

values are found to increase slightly with temperature, D_{min}= 5.12 Å and D_{max}= 5.53 Å (Table 3.2). The temperature dependence of D is shown in Figure 3.6.

The meridional scattering amplitude is obtained from the density variation along the director and gives information about the apparent molecular length, *l*, of the molecules in the nematic phase. In this case unmodified Bragg's relation is used. In BMBT the inner ring is observed to be very weak throughout the nematic phase. So it is very difficult to find the peak positions, necessary to calculate the apparent molecular length (*l*). Only at 165°C, peak positions could be found approximately and corresponding *l* value is found to be 24.3 Å. However, the model length (L) of BMBT in all *trans*-conformation is found to be 26.4 Å. Thus the molecules are tilted at an angle 23.3° at 165°C. Of course, change of conformation of the molecules in the nematic phase may also result in *l* values less than the model length.

In the smectic phase of BBBT the d-spacings corresponding to the intermolecular distances (related to the two outer most rings) do not change appreciably with temperature as shown in Figure 3.7. However, the d-spacing corresponding to the smectic layer spacing (related to the innermost ring) increases with temperature appreciably. If the tilt angle (β_t) of the molecules within the smectic layer is defined as $\beta_t = \cos^{-1}(d/L)$, where d is the layer spacing and L is the model length of the molecules in all *trans* conformations, it is observed that β_t decreases from 33.8° to 24.6° with temperature (Table 3.3). This is shown graphically in Figure 3.8.

The temperature dependence of the average intermolecular distance (D) in the nematic phase of BBBT is shown in Figure 3.9. With temperature D is found to increase slightly, D_{min}= 5.02 Å and D_{max}= 5.24 Å (Table 3.4). On the other hand, it is observed that the value of the apparent molecular length (*l*) increases by 3.7 Å from a value of 22.2 Å to a value of 25.9 Å as the temperature changes from 178°C to 278°C (Table 3.4). This variation is also shown in Figure 3.9. Corresponding change in the tilt angle of the molecules is from 49.8° to 41.1° (Table 3.4), with a mean value of 46.0° and is depicted graphically in Figure 3.10. Value of β_t measured directly from the photograph is found to be about 45° at 183°C, almost

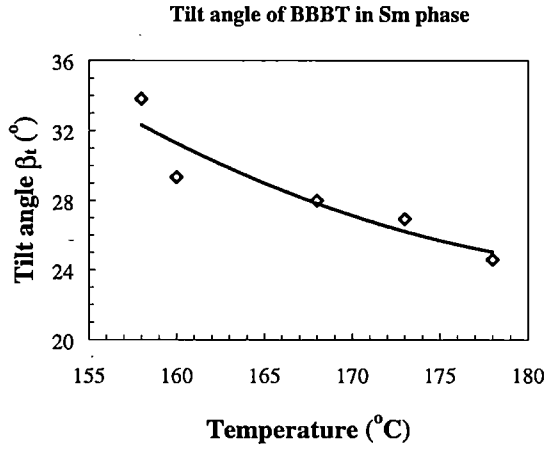

Figure 3.8 Tilt angle β_t (°) as a function of temperature in smectic phase of BBBT.

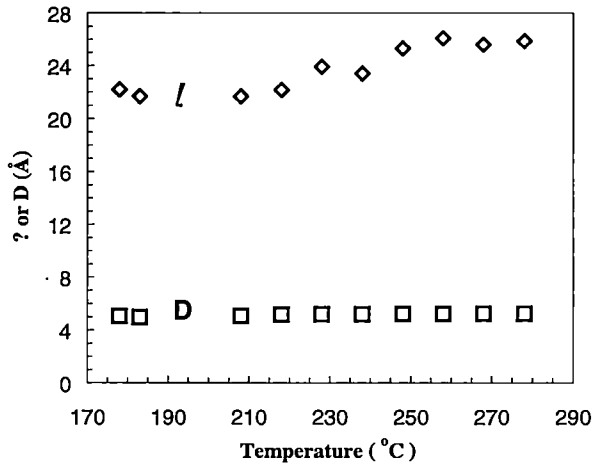

Figure 3.9 Variation of *l* and D with temperature in the nematic phase of BBBT.

equal to the calculated mean value of β_t. However, the tilt angle in this case is almost double the value found in case of BMBT which exhibits an ordinary nematic phase in contrast to the skewed cybotactic nematic phase in BBBT. Following Vainshtein and Chistyakov as described in [35], the size (b) of the cybotactic group was calculated using the relation $b=0.8L/\tan\beta_t$ and found to be about 27 Å. Thus the transverse correlation in the cybotactic group extends not beyond 5 molecular diameters.

Although the nature of temperature variation of the respective molecular parameters *l*, D and β_t is same in the Sm and the N phase, it is observed that there is an abrupt change in those parameters at temperature T_{Sm-N} signifying a first order phase transition. Measured ΔH and ΔS values also support this observation.

Though it is not yet possible to predict with certainty the occurrence of a particular mesophase from the knowledge of the molecular shape and nature of intermolecular interactions, it is argued that knowledge about the molecular packing in the crystalline state may provide an insight in understanding the solid - mesophase transitions [36-38]. It had been shown earlier by co-workers [9] that in the crystalline state BBBT molecules are arranged in layers and within a layer the molecules are tilted with respect to the layer normal. This arrangement is the classical solid state precursor of smectic phase. It may be mentioned here that in BOCP, another di-Schiff's base compound which exhibits only skewed cybotactic nematic phase, parallel imbricated mode of molecular packing was observed [37,39]. For comparison molecular packing diagrams of BBBT and BOCP have been reproduced in Figure 3.11.

Mandal *et al.* [9] observed that BBBT molecules crystallize in triclinic system with cell parameters *a*=6.116Å, *b*=7.916 Å, *c*=31.421 Å and α=92.39°, β=92.35°, γ=96.59° and space group $P\bar{1}$. Also, it is found that the molecular long axis, defined as a best fitted line through all the atoms, makes an angle 32° with the layer normal. Comparing these values with the d-values and the tilt angle of the molecules in the smectic phase it may be inferred that Crystal-Smectic transition is essentially of displacive type [40] contrary to reconstitutive type usually observed at this transition.

In order to get an idea about the intermolecular forces responsible for mesophase stability, all the intermolecular distances less than 3.65Å were calculated. Distances between few carbon atoms of centro-symmetrically related molecules are found to be less than the sum of their van der Waals' radii. Packing fraction of the structure, calculated using method of Kitaigorodsky [41], is found to be 0.73. It may thus be inferred that dispersion forces resulting from van der Waals

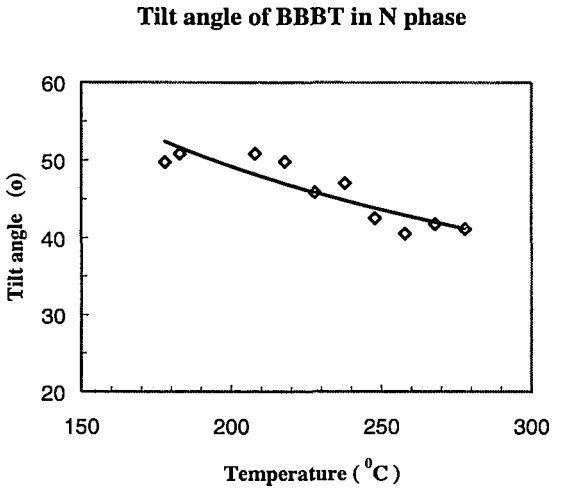

Figure 3.10 Tilt angle β_t (°) as a function of temperature in nematic phase of BBBT.

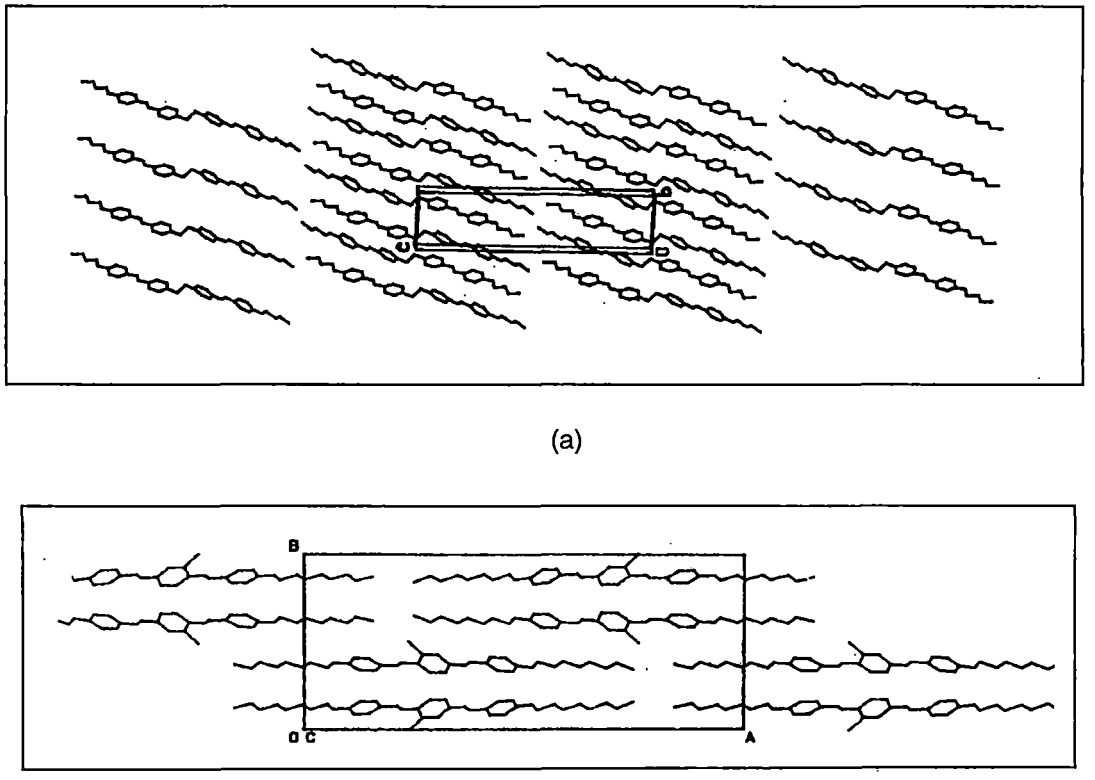

Figure 3.11 Crystal structure of (a) BBBT viewed along X-axis and (b) BOCP viewed along Z-axis.

interactions give rise to very efficient packing of the molecules. High melting point and very large thermal stability of the mesophases may be the result of this packing. No intermolecular contact is found to exist between the transverse dipole moments though the tilting of the molecules within the smectic layers may be favoured by the longitudinal component of the dipoles [42].

Both the orientational order parameters, $\langle P_2 \rangle$ and $\langle P_4 \rangle$, have been determined in the nematic phase by measuring the circular intensity distribution at the peak position of the equatorial crescents. The detailed procedure is given in Chapter II. Measured intensity values $I(\psi)$ as a function of ψ are fitted to an even-powered cosine series (equation 2.18). It is observed that with 8 terms in the series the fitting is quite good. The orientational distribution function f (β) is calculated from the fitted $I(\psi)$ values using equations (2.19) and (2.20) in Chapter II. Measured and fitted intensity values $I(\psi)$ as a function of ψ and the distribution function $f(\beta)$ as a function of β are presented in Table 3.5 for BBBT at temperature of 183°C. Variation of measured and fitted $I(\psi)$ with ψ has been shown in Figure 3.12(a) and that of $f(\beta)$ against β in Figure 3.12(b) at this temperature. As a representative set the observed and fitted $I(\psi)$ as well as the calculated $f(\beta)$ values have been presented only for one temperature (183°C). For brevity these quantities will not be shown even in subsequent chapters.

The temperature variations of the calculated order parameters, $\langle P_2 \rangle$ and $\langle P_4 \rangle$, in N phase of BMBT and BBBT have been shown in Figure 3.13 (and in table 3.6) and Figure 3.14 (and in table 3.7) respectively. Order parameter values were also calculated according to Maier and Saupe [43] mean field theoretical approach (using equation 2.3) and have been depicted in the above figures for comparison. In BMBT both the order parameters are not found to be in good agreement with the MS values. On the other hand, for BBBT, it is seen that $\langle P_2 \rangle$ values agree nicely with theoretical values, however, $\langle P_4 \rangle$ values at higher temperatures are found to be significantly lower than the theoretical values. Such behaviour of $\langle P_4 \rangle$ has been observed in mono-Schiff's base compounds BBBA and APAPA [19,44] and in several other compounds of different molecular structures [45-49]. This discrepancy

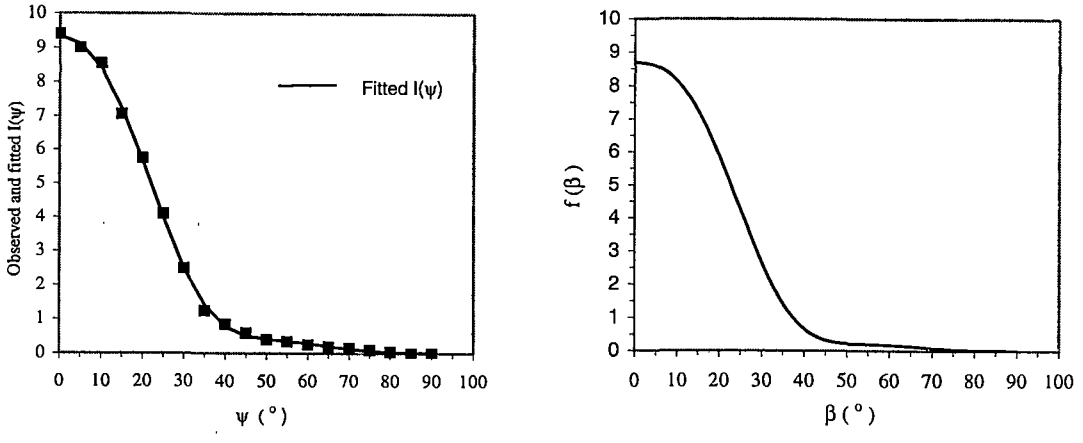

(a) (b)

Figure 3.12 Plot of (a) observed and fitted intensities I(ψ) against ψ and (b) distribution function f(β) against β of BBBT in N phase at 183°C.

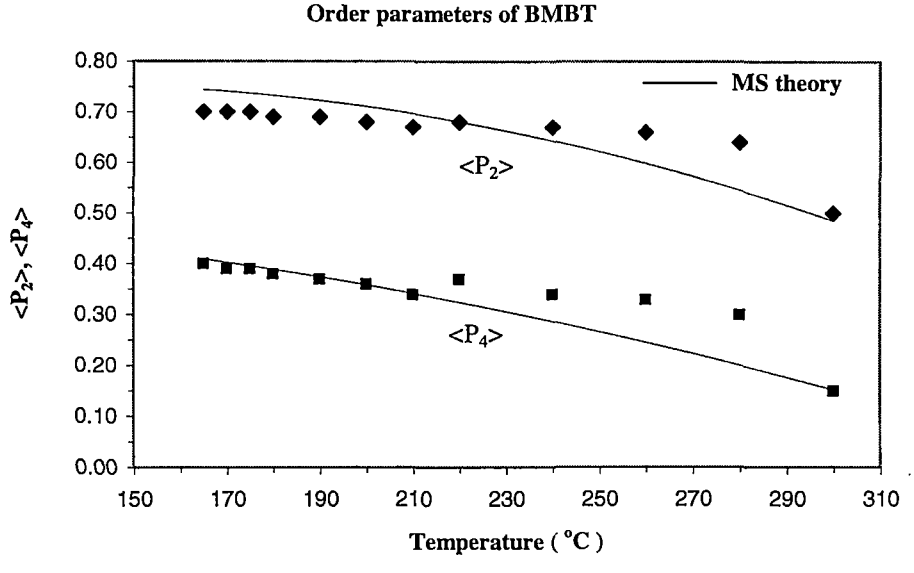

Figure 3.13 Experimental and theoretical order parameters $\langle P_2 \rangle$ and $\langle P_4 \rangle$ plotted against temperature in N phase of BMBT.

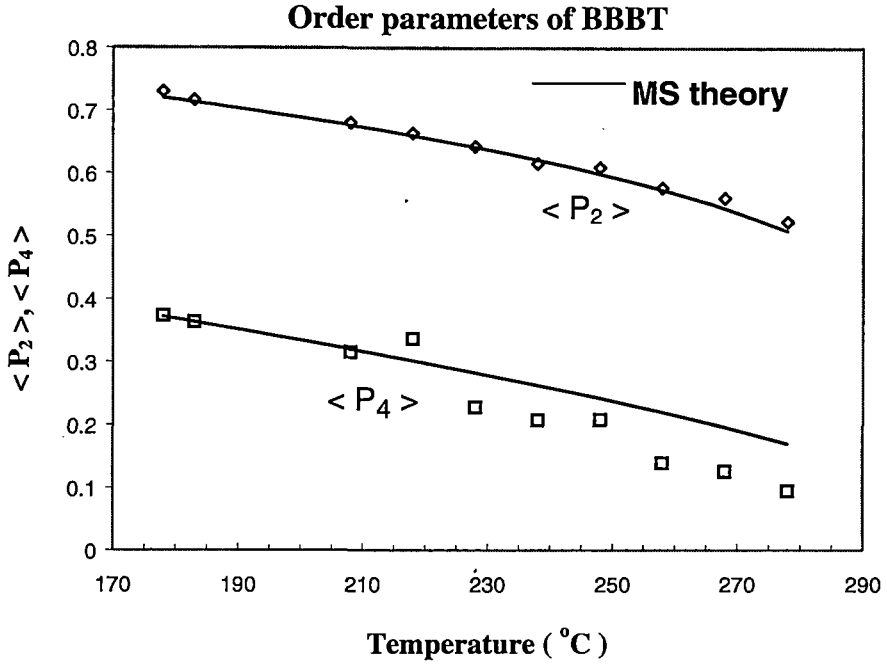

Figure 3.14 Variation of orientational order parameters with temperature in N phase of BBBT.

remains unexplained. According to Faber's continuum theory [50] the parameter $\ln\langle P_2\rangle/\ln\langle P_4\rangle$ should have a universal value of 0.30. In case of BMBT it varies from 0.37-0.39 with mean value of 0.38 whereas in BBBT it varies from 0.27-0.32 with mean value of 0.30 (the value 0.39 at 218°C is ignored). Thus excellent agreement is observed in BBBT but in BMBT the agreement is not good though the values are less spread in this case. Paul [51] and Parimal Sarkar *et al.* [52] also showed that for a large number of nematic compounds the agreement is impressive.

J. W. Goodby [17] has commented that for a typical nematic phase the order parameter has a value in the region of 0.4 - 0.7. Obviously, value of $\langle P_2\rangle$ has been referred here. Order parameters determined for a large number of compounds [51] from this laboratory agree with that observation but values higher than 0.60 are rare. In the two mono-Schiff's base compound APAPA [44] and BBBA [19] the $\langle P_2\rangle$ values are respectively found to be in the range 0.49 - .60 and 0.52-0.61. Range of $\langle P_2\rangle$ values in case of BMBT and BBBT are respectively 0.50-0.70 and 0.52-0.73. Comparable values of $\langle P_2\rangle$ were found in the cybotactic nematic phase of BHeCP,

BOCP and BdeCP [39]. The respective ranges are: 0.55-0.70, 0.60-0.74 and 0.56-0.72. But melting point of these materials is below 100°C. It may be reasonably assumed that high order parameter values of BMBT and BBBT increase their ability in GLC phase separation, as noted in the introduction. High melting point and quite a long range of the nematic phase stability (more than 100°C) are added advantage. Since the order parameters of BBBT are of higher value than those of BMBT, the former may be more effective in GLC separation technique than the latter.

TABLE 3.1

d-spacings of BBBT within smectic phase.

Sample to film distance =4 .92 cm
Wavelength of X-ray used λ=1.5418 Å
Measurements made on aligned sample

Temperature (in °C)	d-spacings (in Å) (Outermost ring is labeled as ring 1)					
	Ring 1	Ring 2	Ring 3	Ring 4	Ring 5	Ring 6
158	4.39	4.55	11.58	14.33	21.34	28.50
160	4.44	4.55	11.97	13.55	21.47	29.90
168	4.50	4.62	12.05	13.80	21.75	30.29
173	4.50	4.68	12.10	15.32	21.29	30.58
178	4.56	4.68	12.22	14.68	22.05	31.19

TABLE 3.2

Intermolecular distances (D) in nematic phase of BMBT

Sample to film distance = 6.92 cm
Wavelength of X-ray used λ=1.5418 Å
Measurements made on aligned sample

Temperature in °C	Intermolecular distance D in Å
165	5.12
170	5.15
175	5.17
180	5.15
190	5.17
200	5.20
210	5.24
220	5.27
240	5.27
260	5.27
280	5.29
300	5.53

TABLE 3.3

Tilt angle (β_t) of BBBT in smectic phase.
Model length of BBBT molecule L=34.3Å

Temperature in °C	Tilt angle β_t in degrees
158	33.8
160	29.3
168	28.0
173	26.9
178	24.6

TABLE 3.4

Intermolecular distance (D), apparent molecular length (*l*)
and tilt angle (β_t) of BBBT in N phase.

Sample to film distance =4.92 cm Wavelength of X-ray used λ=1.5418 Å

Temp. in °C	D in Å	*l* in Å	β_t in degrees
178	5.02	22.2	49.7
183	4.99	21.7	50.8
208	5.04	21.7	50.8
218	5.13	22.1	49.8
228	5.16	23.9	45.8
238	5.18	23.4	47.0
248	5.21	25.3	42.5
258	5.2	26.1	40.5
268	5.23	25.6	41.8
278	5.24	25.9	41.1

TABLE 3.5

Observed and fitted intensities I(ψ) and orientational distribution functions f(β)
Sample: BBBT Temperature: 183°C

Azimuthal angle ψ (°)	X-ray intensity I(ψ) (arbitrary unit)		Orientational angle β (°)	Orientational distribution function f(β) (arbitrary unit)
	Measured	Fitted		
0	9.40	9.34	0	8.70
5	9.00	9.11	5	8.58
10	8.55	8.41	10	8.15
15	7.05	7.23	15	7.27
20	5.75	5.68	20	5.90
25	4.10	4.00	25	4.26
30	2.50	2.50	30	2.66
35	1.25	1.42	35	1.42
40	0.85	0.79	40	0.66
45	0.60	0.51	45	0.32
50	0.40	0.42	50	0.22
55	0.35	0.36	55	0.20
60	0.25	0.29	60	0.17
65	0.20	0.21	65	0.13
70	0.15	0.13	70	0.08
75	0.10	0.07	75	0.04
80	0.05	0.04	80	0.02
85	0.00	0.02	85	0.01
90	0.00	0.02	90	0.01

TABLE 3.6

Orientational order parameters of BMBT in N phase

Temperature (°C)	Order parameters from X-ray data		Maier-Saupe theoretical order parameters	
	$\langle P_2 \rangle$	$\langle P_4 \rangle$	$\langle P_2 \rangle$	$\langle P_4 \rangle$
165	0.70	0.40	0.75	0.41
170	0.70	0.39	0.74	0.40
175	0.70	0.39	0.74	0.40
180	0.69	0.38	0.73	0.39
190	0.69	0.37	0.72	0.37
200	0.68	0.36	0.71	0.36
210	0.67	0.34	0.69	0.34
220	0.68	0.37	0.68	0.32
240	0.67	0.34	0.65	0.29
260	0.66	0.33	0.60	0.25
280	0.64	0.30	0.55	0.20
300	0.50	0.15	0.48	0.15

TABLE 3.7

Orientational order parameters of BBBT in N phase

Temperature in °C	Order parameters from X-ray data		Maier-Saupe theoretical order parameters	
	<P2>	<P4>	<P2>	<P4>
178	0.73	0.37	0.72	0.37
183	0.72	0.36	0.71	0.36
208	0.68	0.32	0.68	0.32
218	0.66	0.34	0.66	0.30
228	0.64	0.23	0.64	0.28
238	0.62	0.21	0.62	0.26
248	0.61	0.21	0.60	0.24
258	0.58	0.14	0.57	0.22
268	0.56	0.13	0.54	0.20
278	0.52	0.09	0.51	0.17

REFERENCES

1. H. Kelker and E.Von Schivizhoffen, *Advances in chromatography*, Vol. 6,(J. C. Giddings and R. A. Keller, Eds.), Marcel Dekker, N. Y., 1968, p. 247.
2. J. P. Schroeder, *Liquid Crystals and Plastic Crystals*, Vol. 1 (G. W. Gray and P. A. Winsor, Eds.), Ellis Harwood, Chichester, England, 1974, p. 356.
3. W. L. Zielinski, Jr., K. Johnston and G. M. Muschik, *Anal. Chem.*, **48**, 907 (1976).
4. M. Hall and D. N. B. Mallen, *J. Chromatog.*, **118**, 268 (1976).
5. P. E. Strup, R. D. Giammer, T. B. Stanford and P. W. Jones in *Carcinogenesis - A comprehensive Survey*, Vol. 1 (R. Freudenthal and P. W. Jones, Eds.), Raven Press, N. Y., 1976.
6. G. M. Janini, K. Johnston and W. L. Zielinski, Jr., *Anal. Chem.*, **47**, 670 (1975).
7. G. M. Janini, G. M. Muschik and W. L. Zielinski, Jr., *Anal. Chem.*, **48**, 809 (1976).
8. G. M. Janini, G. M. Muschik and C. M. Hanlon, *Mol. Cryst. Liq. Cryst.*, **53**, 15 (1979).
9. P. Mandal, S. Paul, K. Goubitz and H. Schenk, *Mol. Cryst. Liq. Cryst.*, **258**, 209 (1995).
10. J. P. F. Lagerwall, P. Rudquist, S. T. Lagerwall and F. Giebelmann, *Liq. Crystals*, **30**, 399(2003)
11. N. Barall II and J. Johnson, *Liquid Crystals and Plastic Crystals*, Vol. 2 (G. W. Gray and P. A. Winsor, Eds.), Ellis Harwood, Chichester, England, 1974, p 255.
12. S. Chandrasekhar, *Liquid Crystals*, 2nd Ed., *Cambridge*, UK, 1992, p26.
13. H. Arnold, *Z. Phys. Chem.*, (Leipzig), **226**, 146 (1964).
14. J. Doucet, The Molecular Physics of Liquid Crystals (G. R. Luckhurst and G. W. Gray, Eds.), Academic Press, London, 1979, p 317.
15. G. Vertogen and W. H. de Jeu, *Thermotropic Liquid Crystals, Fundamentals*, Springer Verlag, Berlin, 1987, p 45.
16. P. S. Pershan, *Structure of Liquid Crystal Phases*, World Scientific, USA, 1988, p 62.
17. J. W. Goodby, *Handbook of Liquid Crystals, Low Molecular Liquid Crystals I*, Vol. 2A (D. Demus, J. Goodby, G. W. Gray, H. W. Spiess and V. Vill, Eds.), Wiley-VCH, Weinheim,1998, Ch. I., p3.
18. L. Richter, D. Demus and H. Sackmann, *J. Phys. (Paris)*, **37**, C3-41 (1976).
19. P. Mandal, M. Mitra, S. Paul and R. Paul, *Liquid Crystals*, **2**, 183 (1987)
20. D. Demus, S. Diele, M. Klapperstuck, V. Link and H. Zaschke, *Mol. Cryst. Liq. Cryst.*, **15**, 161 (1971).
21. J. Doucet, A. M. Levelut and M. Lambert, *Mol. Cryst. Liq. Cryst.*, **24**, 317 (1974)
22. J. Doucet, A. M. Levelut and M. Lambert, *Phys. Rev. Lett.*, **32**, 301 (1974).
23. P. Mandal, R. Paul and S. Paul, *Mol. Cryst. Liq. Cryst.*, **131**, 299 (1985).
24. D.S. Hulme and E.P. Raynes, *J. Chem. Soc., Chem. Commun.*, 98 (1974).
25. K. Hori and H. Wu, *Liquid Crystals*, 26, 37 (1999).
26. K. Hori, M. Kurosaki, H. Wu and K. Itoh, *Acta Cryst.*, C52, 1751 (1996).
27. M. Kuribayashi and K. Hori, *Liquid Crystals*, 26, 809 (1999).
28. A. Jakli, I. Janossy and A. Vajda, *Liquid Crystals*, **27**, 1035(2000).
29. A. de Vries, *Mol. Cryst. Liq. Cryst.*, **10**, 31 (1970).

30. A. de Vries, *Mol. Cryst. Liq. Cryst.*, **10**, 219 (1970).

31. A. de Vries, *Liquid Crystals, The Fourth State of Matter* (F. D. Saeva, Ed.), Marcel Dekker, New York, 1979, p. 15.

32. L. V. Azaroff, *Proc. Nat. Acad. Sci.*, **77**, 1252 (1980).

33. V. M. Sethna, A. de Vries and N. Spielberg, *Mol. Cryst. Liq. Cryst.*, **62**, 141 (1980).

34. L. V. Azaroff and C. A. Schumann, *Mol. Cryst. Liq. Cryst.*, **122**, 309 (1985).

35. Parimal Sarkar, Pranab K. Sarkar, Sukla Paul and Pradip Mandal, *Phase Transitions*, **71**, 1 (2000).

36. R. F. Bryan, *J. Struc. Chem.*, 23, 128(1982).

37. P. Mandal, S. Paul, H. Schenk and K. Goubitz, *Mol. Cryst. Liq. Cryst.*,**210**, 21 (1992) and references therein.

38. W. Haase and M.A. Athanassopoulou, *Liquid Crystals*, D.M.P. Mingos(Ed.), Springer-Verlag, Vol. I, pp. 139-197 (1999).

39. B. Jha, S. Paul, R. Paul and P. Mandal, *Phase Transitions*, **15**, 39(1989).

40. R. F. Bryan and P. G. Fourier, *Mol. Cryst. Liq. Cryst.*, **60**, 133 (1980).

41. A. I. Kidaigorodsky, *Molecular Crystals and Molecules*,Academic Press, New York, 1973, p 18.

42. N. V. Madhusudana, *Liquid Crystals —Applications and Uses* (B. Bahadur, Ed.), World Scientific, Singapore, 1990, p. 76.

43. W. Maier and A. Saupe, *Z. Natureforsch.*, **14a**, 882 (1959); Ibid, **15a**, 287 (1960).

44. P. Mandal, M. Mitra, K. Bhattacharjee, R. Paul and S. Paul, *Mol. Cryst. Liq. Cryst.*, **149**, 203 (1987).

45. B. Bhattacharjee, S. Paul and R. Paul, *Molec. Phys.*, **44**, 1391 (1981).

46. B. Bhattacharjee, S. Paul and R. Paul, *Mol. Cryst. Liq. Cryst.*, **89**, 181 (1982).

47. S. Jen, N. A. Clark, P. S. Pershan and E. B. Priestley, *Phys. Rev. Lett.*, **31**, 1552 (1973)

48. S. Kobinata, Y. Nakajima, H. Yoshida and S. Maeda, *Mol. Cryst. Liq. Cryst.*, **66**, 387 (1981)

49. J. P. Heagen, *J. Phys. Lett. (Paris)*, **36**, 209 (1975).

50. T. E. Faber, *Proc. Royal Soc. London A*, **353**, 247(1977).

51. R. Paul, *Liquid Crystals*, **9**, 239 (1991).

52. P. Sarkar, P. Mandal, S. Paul, R. Paul, R. Dabrowski and K. Czyprinski, *Liq. Crystals,* **30**, 507(2003).